INTERACTION OF WHEY PROTEIN WITH MODIFIED STAINLESS STEEL SURFACES

S.S. Premathilaka[1a], M.M. Hyland[1b], X.D. Chen[1c], L.R. Watkins[2], and B. Bansal[1*]

[1] The Department of Chemical and Materials Engineering, The University of Auckland Private Bag 92019, Auckland 1142 NEW ZEALAND

[a] sram036@ec.auckland.ac.nz; [b] m.hyland@auckland.ac.nz; [c] dong.chen@eng.monash.edu.au

[2] Department of Physics, University of Auckland, Private Bag 92019, Auckland 1142 NEW ZEALAND

l.watkins@auckland.ac.nz

ABSTRACT

Modified stainless steel surfaces were fouled with whey protein solutions to study the deposition mechanisms and the effects of surface modification. Stainless steel samples were coated with diamond-like carbon (DLC) and titanium nitride (TiN). These surfaces are expected to present different surface chemistries to stainless steel in terms of their functional groups and hydrophobic or hydrophilic nature. Thus, it is expected that foulant-surface interactions will differ for the various fouled surfaces.

The substrates were exposed to a flowing whey protein solution in a fouling rig designed to achieve laminar flow. X-ray Photoelectron Spectroscopy (XPS) was used to study the initial protein-surface interactions of samples fouled for 1 minute at 75°C. Ellipsometry was used to study the fouling and cleaning performance of samples fouled at 75°C and 85°C for up to 30 minutes followed by ultrasonic caustic cleaning of selected samples.

XPS showed the presence of similar protein functional groups on all fouled surfaces. The bonding mechanisms during fouling of DLC is different to the stainless steel and TiN surfaces. The peptide link played a more active role at the deposit-surface interface for the non-polar DLC surface, while it was less significant for the two polar surfaces. Ellipsometry revealed that for the three surfaces, fouling increased in the order DLC<SS<TiN, and cleanability increased in the order TiN<SS<DLC. Furthermore, the nature of the surface influenced the structure of the deposit after the initial protein layer was formed.

It was concluded that the surface chemistry can influence the deposition mechanisms in terms of the orientation of protein functional groups as well as the amount of fouling, the structure of the deposit and hence the deposit removal behaviour.

INTRODUCTION

Dairy fouling has been studied by many researchers around the world for over 50 years. Various approaches have been used in these investigations to more clearly understand the underlying mechanisms that lead to fouling.

Such studies involve the analysis of both general fouling parameters such as the change in fouling resistance or pressure drop with time (Deplace et al. 1994; Changani et al. 1997; Muller-Steinhagen et al. 1997; Robbins et al. 1999), and more specific measurements to further clarify the processes that take place during deposition (Britten et al. 1988; Brassart 1990; Elofsson et al. 1996; Sakiyama et al. 1999; Rosmaninho et al. 2003; Parbhu et al. 2004; Liu et al. 2006; Santos et al. 2006).

Some recent studies have focused on modifying the stainless steel surface as a method to reduce the effects of milk fouling (Britten, Green et al. 1988; Muller-Steinhagen and Zhao 1997; Bornhorst et al. 1999; Zhao et al. 2004; Zettler et al. 2005; Santos, Nylander et al. 2006; Rosmaninho et al. 2007). In this study it is believed that the effect of surface modification is most clearly understood during the initial stages of fouling. Recent results obtained from the analysis of the effect of the surface on the first few minutes of whey protein fouling are presented. The change in surface chemistry as a result of modification, and the influence this has on deposition forms the basis of this investigation. Unmodified stainless steel, and stainless steel coated with titanium nitride (TiN) and diamond-like carbon (DLC) are studied. X-ray Photoelectron Spectroscopy (XPS) is used to study the fouling mechanisms by identifying possible protein functional groups that take part in bonding with the surface. Ellipsometry is used to determine the deposit mass formed after a certain period of time.

Both TiN and DLC have been used for biological implants, and the interactions of these materials with proteins and bodily fluids has been studied in some detail (Kola et al. 1996; Grill 2003; Hauert 2003; Park et al. 2003; Piscanec et al. 2004; Sheeja et al. 2004). DLC is a low surface energy material, and its surface chemistry can easily be modified by doping it with suitable elements (Grill 1999; Peters et al. 2003; Trippe et al. 2004). TiN coatings have been used for various applications in the past (Sundgren 1985; Milosev et al. 1994; Valvoda 1996; Fortuna et al. 2000; Zhao et al. 2000), and their surface chemistry is generally well understood.

[*] Current Address: Fonterra Co-operative Group Ltd Dairy Farm Road, Private Bag 11029,Palmerston North, New Zealand. Email: bipan.bansal@fonterra.com

MATERIALS AND METHODS

Fouling Rig

Figure 1 shows the set up of the experiment used for fouling. The fouling module was designed to accommodate small samples that could be easily installed for deposit formation, and removed for drying and analysis. The purpose of this was to eliminate any damage imposed to the deposit structure and topography as a consequence of cutting to dimensions required by the various analysis techniques. The module is essentially an electrically heated and insulated tube with rectangular cross section. The inlet and outlet have been tapered to allow for entrance and exit effects as the fluid passes through. The sample area allows for mounting of samples to be flush with the surface so as to minimize turbulence. The base material for all samples is stainless steel. As shown in Figure 1, thermocouples are placed to detect the bulk liquid temperature, and the stainless steel surface temperatures along the sample area. In this way it was possible to visualize the temperature distribution through the rig during heating and during an experiment.
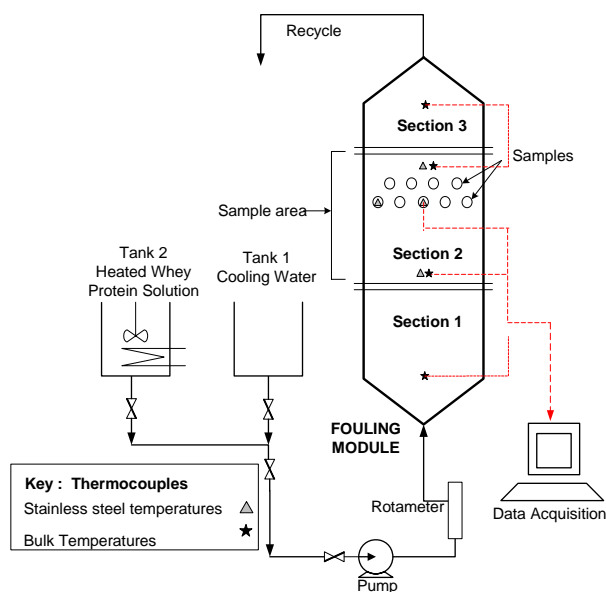

Figure 1: Schematic of Fouling Rig

Fouling Experiments

Fouling experiments were performed at temperatures of 75°C and 85°C with whey protein isolate (WPI) concentrations of 6g/L and 15g/L. For XPS studies, it was important to study the first few layers of protein, and hence fouling was performed at 75°C with a WPI concentration of 6g/L for a period of 1 minute. It was expected that at these conditions, the foulant layer would be sufficiently thin to allow detection of the interface between the deposit and the surface. For ellipsometry analysis of fouling performance for each of the three coatings, firstly, the initial fouling behaviour was studied. This was achieved by fouling at 75°C with a WPI concentration of 6g/L and fouling times of 3, 6, and 10 minutes. Secondly, it was required to observe fouling after the initial stages. Accordingly, the fouling temperature and WPI concentration were increased to 85°C and 15g/L respectively, and fouling times of 10, 20, and 30 minutes were used.

During a fouling experiment, the whey protein solution heated to 75°C or 85°C was pumped through the fouling module which was also heated to the same temperature. Once the fouling time was reached, cooling water was pumped through the rig for 120 seconds to quench the fouling reaction and to remove any loosely bound particles deposited on the surface. This extended quenching time was also required to ensure protein material did not contact the sample when draining. At shorter quenching times a protein foam was found to contact the sample while draining and this was not desired. Once drained, the samples were removed and dried overnight for XPS and ellipsometry analysis.

Cleaning Experiments

The samples fouled at 75°C for 6 and 10 minutes were cleaned after measuring the adsorbed mass during fouling. Firstly, the samples were ultrasonically cleaned at 60Hz in a 0.5wt% NaOH solution heated to 60°C, for 2 minutes. This was followed by a second ultrasonic clean in distilled water at room temperature for 1 minute. The samples were dried overnight before ellipsometry measurements.

Fouling Solutions

Whey protein solutions were prepared by reconstituting whey protein isolate powder (ALACENTM 894 provided by Fonterra Co-operative Group Limited, Te Rapa), which contains approximately 90% whey proteins, to a concentration of 6g/L. This concentration was chosen as it represents the concentration of whey proteins in milk (Walstra et al.,1984). For ellipsometry studies a higher concentration of 15g/L was also used to obtain a thicker deposit.

Sample Materials

The stainless steel substrates were made from 304SS, subsequently polished to 0.25micron. The samples were 10mm in diameter and 5mm thick. 304SS is the preferred type of stainless steel used in New Zealand dairy plants, and was thus the choice for this research. DLC coatings were obtained from Bekaert Advanced Coatings, Belgium, and TiN coatings were obtained from

Surface Technology Coatings, Australia. DLC coatings were produced by chemical vapour deposition (CVD) resulting in a hydrogen containing DLC structure. TiN coatings were produced by low voltage electron beam technology.

ANALYSIS TECHNIQUES

X-ray Photoelectron Spectroscopy

XPS is a semi-quantitative surface characterization technique. The sample surface is bombarded with x-rays resulting in the removal of electrons from atoms in the material. The binding energy of the ejected electrons is calculated and can be used to determine the element present and its chemical state. A wide scan provides the elemental composition of the surface in general. A narrow scan gives more specific information on the percentages of different chemical states of the same element. Quantification of the obtained spectra was performed using CASAXPS. The software uses the peak area and sensitivity factors to evaluate the relative atomic percent of each peak. The XPS used for this study was a Kratos Axis DLD with a hemispherical analyser. The estimated analysis depth is 1 - 2nm. The x-ray source was mono-chromatised Al Kα, and the analyser resolution was 1% of the pass energy. For elemental analysis a pass energy of 160eV was used, while 10eV was used for narrow scans. The binding energy calibrants were Au4f and Cu2p for span of peak positions, and Ag3d for absolute peak positions. The system pressure was 10^{-9}Pa. Charge neutralization was not used during analysis. Correction for shifts in binding energies due to charge accumulation on the surface was performed by referencing to C-C/C-H bonds (hydrocarbons) at 285.0eV.

Ellipsometry

Ellipsometry is a non-contact optical technique t used to determine the properties of substrates and films. The change in polarisation that occurs on reflection of polarised light from a sample is measured and used to infer either the refractive index, n, of a substrate, or the thickness, d, and refractive index of a film. The instrument used for these studies was a null ellipsometer, operating at 632.8 nm (HeNe laser) using angles of incidence between 50° to 70°. Here, the angle of incidence is measured with respect to the normal to the sample surface. The instrument returns two angles Ψ and Δ which, for each angle of incidence, were calculated using four-zone averaging (Azzam et al. 1977) as this yields the most accurate results. The unfouled substrates (SS, TiN and DLC) were measured at 60° angle of incidence and the measured ellipsometric angles were

used to calculate their respective complex refractive indices directly (Azzam and Bashara 1977). Fouled surfaces were measured at three different angles of incidence at each angle to calculate Ψ and Δ. A three layer, air-film-substrate model, with the refractive index and thickness (n, d) of the film as variable parameters, was used to calculate ellipsometric angles at each of the experimental angles of incidence. A non-linear fitting program searched for values of n and d that minimized the sum of the mean square differences between the measured and calculated ellipsometric angles.

The values obtained for n and d using this program were used to determine the deposit mass using Equation 1 (Cuypers et al. 1984), which describes the mass of an adsorbed layer of thickness, d, and refractive index, n; where, Γ is the deposit mass in mg/m², d is the deposit thickness in nm, n is the refractive index of the film or deposit, M/A is the ratio of the molar weight to the molar refractivity of the whey protein and is equal to 4.1g/ml (Santos et al. 2006).

$$\Gamma = \frac{Md}{A}\left(\frac{n^2-1}{n^2+2}\right) \tag{1}$$

XPS ANALYSIS OF INITIAL DEPOSITION MECHANISMS

Unfouled Surfaces

SS, TiN and DLC surfaces were analyzed to first determine the substrate surface chemistry. This was expected to provide an indication of possible bonding behaviour with the protein molecules. Figure 2a shows a wide scan of a typical stainless steel surface before fouling. Removal of the contaminating C layer by Argon sputtering (spectrum not shown here) showed an increase in the stainless steel elements of Fe, Cr, and Ni, accompanied by a decrease in O, which confirmed the presence of an oxide layer known to form on metal surfaces exposed to atmosphere. The narrow scans revealed two O components corresponding to Fe and/or Cr oxides at 530.1eV (Moulder et al. 1992), and metal hydroxides and C-O bonds at 531.8eV. C-O bonds were present due to surface contamination. The contaminating C layer consisted of three components, the major functional group being C-C/C-H bonds (285.0eV). Small amounts of metal carbides (284.4eV) and C-O groups (286.1eV) (Beamson et al. 1992) were also detected.

The TiN surface is comprised of the elements Ti, N, O, and C (Figure 3a). Analysis of the Ti $2p_{3/2}$ narrow scan (not shown here) showed that three titanium components were present, corresponding to TiN at 455.2eV (Milosev et al. 1995; Lu et al. 1999), TiO_2 at 458.4eV (Lu and

Chen 1999; Georgiev et al. 2004; Zhang et al. 2004), and an intermediate component at 456.5eV described as TiN_xO_y (Bertoti et al. 1995; Lu and Chen 1999; Gyorgy et al. 2003). It is generally understood that the oxide forms the top most layer on TiN coatings. Interstitial N_2 formed during deposition was also detected in small amounts from the N 1s narrow scan. C on the surface was due to contamination in the form of C-C/C-H, C-O, and C=O bonds.

XPS of DLC indicated the presence of only C with a small amount of O due to contamination (Figure 4a). The C 1s spectrum (not shown here) indicated the top most surface layer contained mostly sp^2 bonded carbon (89%) and 9% sp^3 bonded C. An sp^2 rich layer is typically found on DLC surfaces, as these bonds are more thermodynamically stable than the metastable sp^3 bonds (Grill 1999). A small percentage of C-O bonds (contamination) was also detected.

Both the stainless steel and TiN surface chemistries are defined by their oxide layer, and hence polar interactions with the protein are most likely. Such interactions could include bonding with charged groups in the protein, hydrogen bonding between the N-H groups in the protein and the metal oxide, and interactions with carboxyl and hydroxyl groups in the protein. In contrast, the DLC surface can be considered as a hydrophobic surface since it is mainly comprised of C-C and C-H bonds. Thus interactions with this surface are more likely to be with the non-polar chains in the protein.

Fouled surfaces

Wide scans for fouled stainless steel, TiN, and DLC surfaces are shown in Figure 2b, Figure 3b, and Figure 4b respectively. For all cases, the substrate is still detected, indicating that the interface between the deposit and substrate is also detected. The intensity of the C and O peaks are significantly increased and a new N component is detected as a result of protein deposition. To further understand the protein surface chemistry, narrow scans of the C, N, and O peaks were performed. Component identification for the deconvoluted peaks is summarized in Table 1. Narrow scans for C, N, and O for the three surfaces are presented in Figure 5to Figure.

The C1s and N 1s narrows scans were similar for all 3 surfaces, with the exception of TiN where N1 to N3 are substrate components. With respect to the O 1s narrow scan, it was found that while O2 was the major component for the fouled SS and TiN, this was not the case for the fouled DLC. Since all the protein functional groups should be present on each surface, differences in major and minor components could be the result of some groups being buried further into the deposit, and hence contributing less to the overall XPS signal. As such, it can be stated that the peptide or amide group is more active at the interface for the DLC surface than for the SS and TiN surfaces. For the latter surfaces, it appears that the C bonded to O groups play a more significant role at the interface. To further analyse these deposition mechanisms, angle resolved XPS was performed on the fouled TiN and DLC surfaces.

Angle Resolved Analysis

Narrow scans of C, N, O, and Ti (for fouled TiN) were performed for 4 angles of 0°, 15°, 30°, and 45°. The angle is that made between the sample and the detector. At 0° the detector is perpendicular to the sample. Increasing the angle reduces the depth of analysis, which results in detection of components further away from the deposit-surface interface. Figure 8 shows the change in substrate components with the angle of detection. The Ti 2p narrow scans indicated a reduction in TiN and TiNxOy components, with an increase in TiO2. These observations verify protein deposition on TiN takes place via interactions with the oxide layer. In terms of the substrate N components, slight reductions in N1 and N2 were found which agree with the changes seen in the Ti 2p angle resolved results. With regards to the protein components (Figure 9), the main change observed was in the C-C/C-H bonds. This suggests that the non-polar chains in the protein structure are oriented away from the surface. Interestingly, no significant change was observed in the peptide components (C3, O2, or N5). N5 was earlier considered as both C-N groups and peptide groups. If this peak is a result of both these components, then it would be difficult to detect any changes in angle resolved analyses, which is what is observed here.

The TiN coating is comprised of at least 3 layers. It is evident that increasing the angle of detection influences mainly the intensity from these layers rather than the protein layers. Deposits formed with longer fouling times are currently being analyzed to further investigate the trends seen here.

The main changes observed in angle resolved analysis of fouled DLC are summarized in Figure 10 and Figure 11. The functional groups outlined in Table 1 included all the possible groups cited in literature. By examining the trends obtained by angle resolved analysis it was possible to eliminate some of these functional groups, as follows. From the earlier analysis of component identification, the O2 group was determined as peptide groups. These groups were also a possibility for the O3 component along with carboxyl, C-OH, and C-O groups. However, as seen in Figure 10 and 11, O2 decreases in atomic% as the angle is increased, while O3 increases. Thus, O3 cannot be due to peptide groups and is hence due to only O=C-O, C-OH and C-O groups.
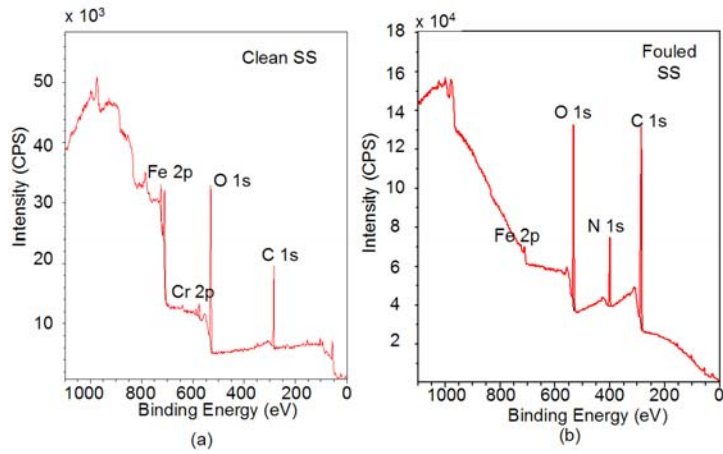
Figure 2: Wide scans of (a) clean stainless steel and (b) fouled stainless steel
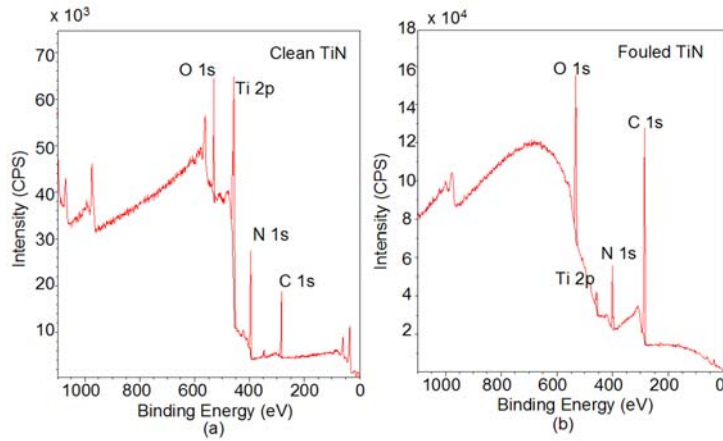
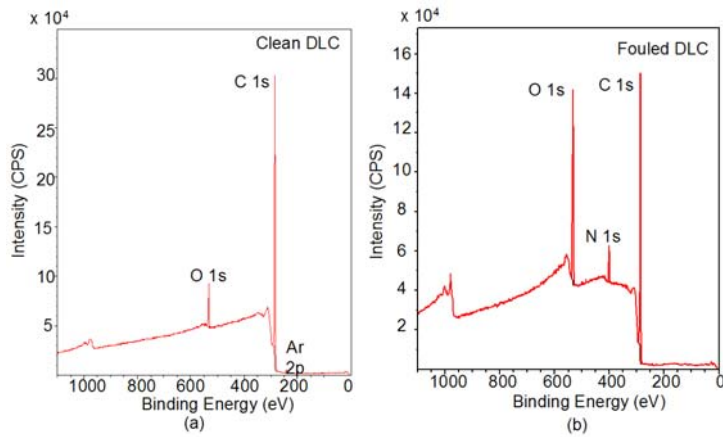Figure 3: Wide scans of (a) clean TiN and (b) fouled TiN

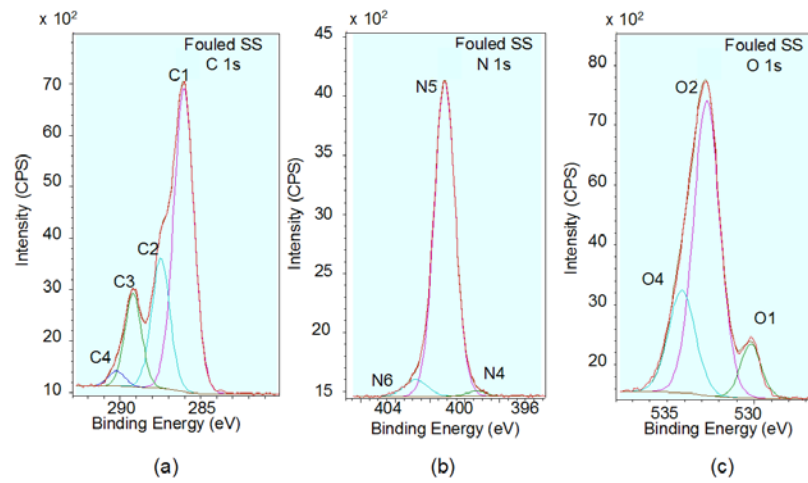Figure 4: Wide scans of (a) clean DLC and (b) fouled DLC

Figure 5: (a) C 1s (b) N 1s, and (c) O 1s narrow scans for stainless steel fouled for 1 minute at 75°C
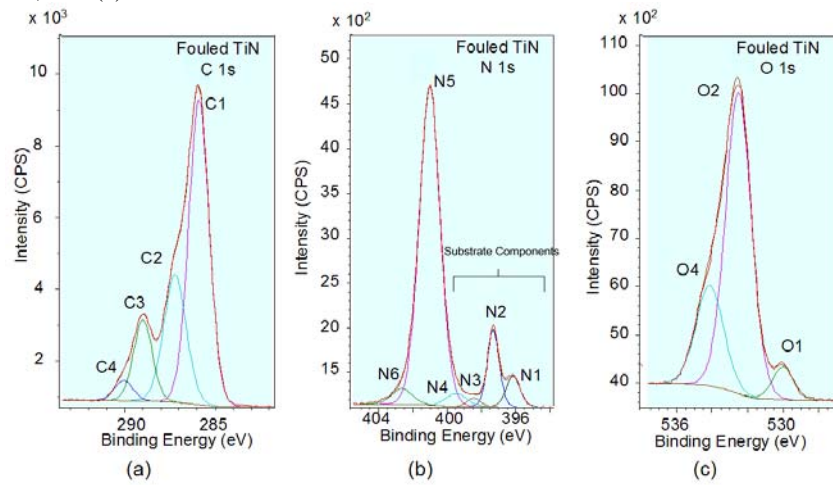

Figure 6: (a) C 1s (b) N 1s, and (c) O 1s narrow scans for TiN fouled for 1 minute at 75°C
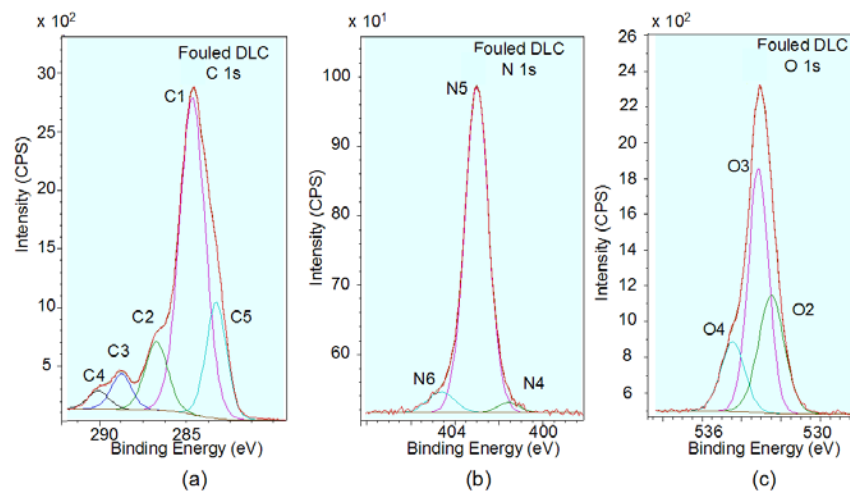

Figure 7: (a) C1s (b) N1s, and (c) O 1s narrow scans for DLC fouled for 1 minute at 75°C

Table 1: Summary of C, N, and O components identified on fouled surfaces

Element	Assignment	BE (eV)	Reference[a]
C	C1: C-C,C-H	285.0	1, 2, 3, 4
	C2: C-O	286.6	1, 4, 5, 6,
	C3: O=C-N (peptide group)	288.0	1, 4, 7, 8
	C4: O-C=O	289.2	5, 9, 10
N	N1: TiN_xO_y	396.1	11, 12
	N2: TiN	397.2 – 397.4	12, 13
	N3: Interstitial N_2	398.5 – 398.6	13
	N4: Interstitial N_2, C-N, O=C-N (peptide bond)	399.3 – 399.7	8, 13, 14, 15
	N5: C-N, O=C-N (peptide bond)	400.0 – 400.1	8, 14, 15
	N6: charged N (-NH$^+$)	401.4 – 401.8	3, 8, 10, 14
O	O1: metal oxide	529.1	1, 8, 14, 16
	O2: O=C-N (peptide bond)	531.7	8, 15, 16
	O3: O=C-N (peptide bond), O-C=O, C-O, C-OH	532.4	3, 16
	O4: adsorbed moisture, O-C=O (carboxyl bond), C-O, C-OH	533.2	6, 7, 16

a. References: 1.(Wei et al. 2003); 2.(Schmidt 2001); 3.(Olivares et al. 2006); 4.(Pradier et al. 2002); 5.(Tidwell et al. 2001); 6.(Beyer et al. 2006); 7.(Zubavichus et al. 2004); 8.(Xiao et al. 1997); 9.(Browne et al. 2004); 10.(Clark et al. 1976); 11.(Milosev, Strehblow et al. 1995); 12.(Lu and Chen 1999); 13.(Bertoti, Mohai et al. 1995); 14.(Vinnichenko et al. 2002); 15.(Petoral Jr. et al. 2002); 16.(Beamson and Briggs 1992)

This suggests that the peptide groups are oriented closer to the interface while the carboxyl, C-O, and C-OH groups are oriented further away from the interface. Again, this agrees with the earlier observation from the O1s narrow scan.N5 was considered to be peptide or C-N groups and shows a slight decrease as seen in Figure 11. Interestingly, no change was observed in the corresponding C component for peptide groups (C3). A change was also expected in the C1 components (C-C/C-H) as these were the main groups expected to interact with the non-polar DLC surface. However no significant change in this component was observed except for a slight increase as a result of the surface carbon contaminating layer.

The angle resolved results for fouled DLC surfaces revealed some key observations. The peptide group appears to play a more significant role in surface bonding while groups with C bonded to O are less active at the interface. These findings agree with the initial speculations from the O1s narrow scans of fouled DLC. As the DLC is a non-polar surface, bonding with the carboxyl or C-O groups is not expected, and this has been verified with this study. It appears that the peptide group takes part during the deposition process, but it is unclear how this takes place. Further analysis using this technique is expected to provide some more insight to this investigation.
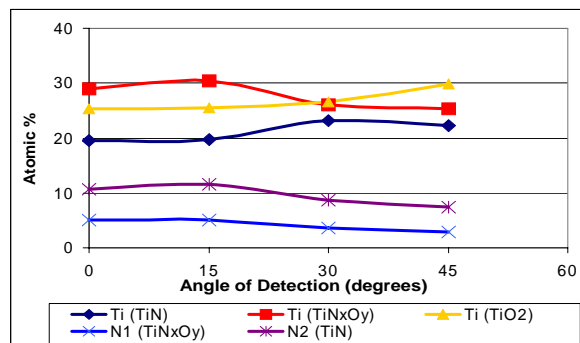

Figure 8: Change in atomic% of substrate components with angle of detection for fouled TiN
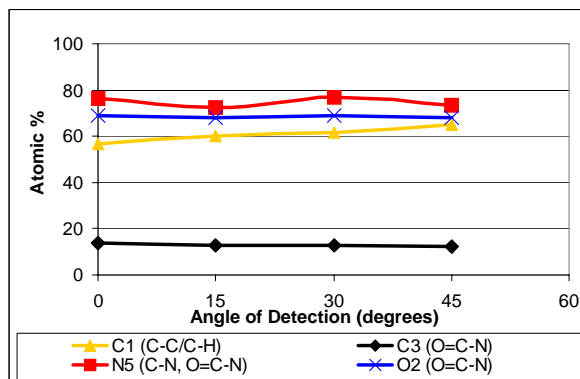

Figure 9: Change in atomic% of deposit components with angle of detection for fouled TiN
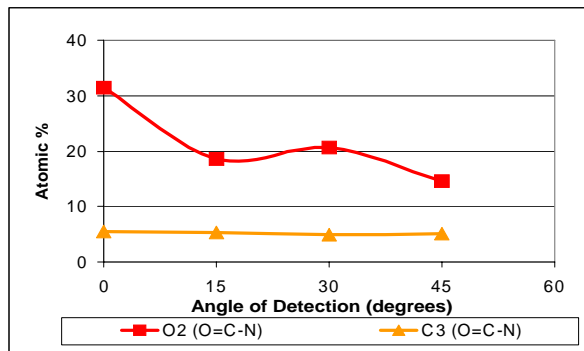
Figure 10: Change in atomic% of deposit components with angle of detection for fouled DLC
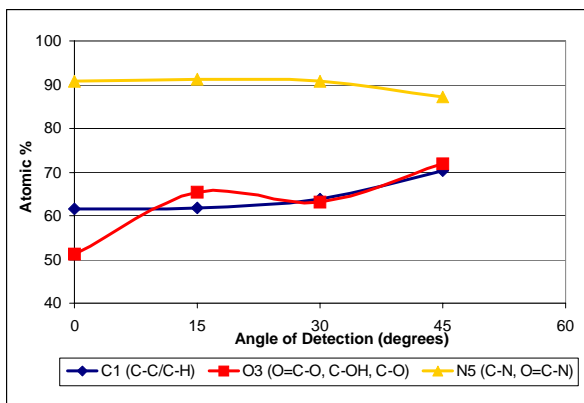

Figure 11: Change in atomic% of deposit components with angle of detection for fouled DLC

ELLIPSOMETRY STUDY

Adsorbed Deposit Mass

The adsorbed deposit mass for stainless steel, TiN and DLC surfaces fouled at 75°C with a WPI concentration of 6g/L are shown in Figure 12. The experimental data for fouling times of 3, 6, and 10 minutes are shown. Some indicative trends of the fouling behaviour for the first 10 minutes are also included in the graph. At t = 0 minutes, the deposit mass is assumed to be 0mg/m^2. It is evident that the DLC surfaces have the lowest degree of fouling. It appears that after the initial level of deposition of approximately 4mg/m2, further deposition does not take place. In contrast, the deposit mass for the TiN surface increases at a constant rate for the first 10 minutes. As such, the degree and rate of fouling for this surface is higher than for the DLC surface. The stainless steel surface initially has a higher level of deposition than both the former surfaces; however the rate of deposition appears to decrease after 3 minutes, resulting in a lower deposition rate than the TiN surface. In Figure 13, the deposit mass for all three surfaces fouled with a WPI solution of 15g/L concentration at 85°C is shown. It should

be noted that the deposit mass values are lower than expected at these conditions, and are quite similar to the values obtained at 75°C. This low deposit mass is most likely due to some removal of the deposit during quenching. Nevertheless, the trends observed from these results can be compared with those in Figure 12, and some important conclusions can be made. At 10 minutes of fouling, the DLC appears to have the least amount of deposition and with increasing fouling time, the deposit mass does not increase significantly. The TiN surface appears to have a constant rate of deposition up to 20 minutes of fouling. Beyond this fouling time, the deposition rate decreases along with some removal of the deposit as well. The rate and amount of fouling for this surface seems to be the highest for all three surfaces. For the stainless steel surface, after 10 minutes of fouling, there is a noticeable reduction in deposit mass, which is most likely due to the removal of deposit during quenching. However, there is no change in deposit mass between 20 and 30 minutes of fouling suggesting that the rate of fouling has decreased.

The adsorbed deposit mass results for both fouling conditions present similar results. It is clear that the overall rate and amount of fouling decreases in the order, TiN>SS>DLC. The apparent removal of deposit at the higher temperature indicates that as the deposit becomes thicker removal becomes easier. The deposit removal behaviour for the three surfaces is investigated further in the next section

Deposit Removal

The samples fouled for 6 and 10 minutes at 75°C were cleaned using the cleaning treatments outlined earlier. Figure 14 compares the percentage of deposit removed after cleaning the three surfaces. It is evident that the TiN surface has the poorest cleanability.
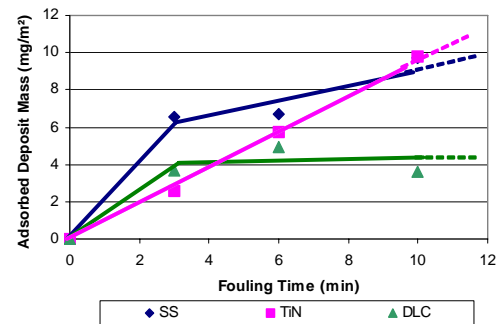

Figure 12: Adsorbed deposit mass for surfaces fouled at 75°C with 6g/L WPI solutions
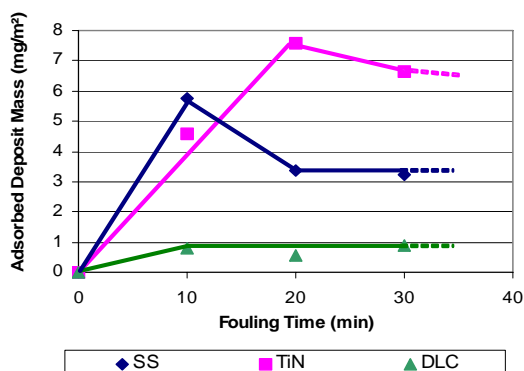
Figure 13: Adsorbed deposit mass for surfaces fouled at 85°C with 15g/L WPI solutions

For the samples fouled for 6 minutes, the DLC appears to have the highest cleanability. For the samples fouled at 10 minutes, this trend is not as clear, however, this is due to the fact that the amount of deposit before cleaning was much higher for the stainless steel than for the DLC surface. Overall, it is clear that the cleanability increases in the order TiN<SS<DLC.
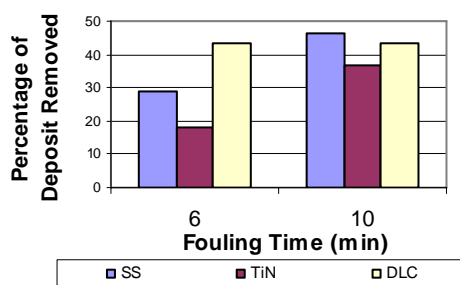

Figure 14: Percentage of Deposit Removed after cleaning SS, TiN and DLC surfaces fouled at 75°C for 6 and 10 minutes

In Figure 15 and Figure 16 the deposit mass before cleaning is compared with the deposit mass removed after cleaning. It can be seen that for the same initial deposited mass, the deposit mass removed is different. In Figure 15, this is shown by the TiN and DLC surfaces, and in Figure 16, this is shown by the TiN and SS surfaces. Furthermore, for all surfaces, more than 50% of the deposit still remained after the cleaning treatment. As such, the cleaning treatment can be viewed as removal of mainly the outer layers of the deposit, leaving a strongly adhering layer on the surface. This suggests that the structure of the deposit after the initial layer is different for the three surfaces, resulting in varying levels of deposit removal when the mass before cleaning was relatively similar. This result agrees with Rosmaninho et al (2007) where similar comparisons of the mass before

fouling and the mass removed revealed that the deposit structure was different on surfaces of varying surface energies. Hence, while the type of surface can influence the deposit-surface interactions, it also influences the deposit-deposit interactions.
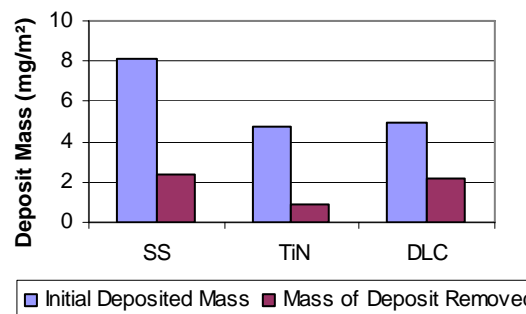

Figure 15: Deposit mass before and after cleaning for SS, TiN & DLC surfaces fouled at 75°C for 6min
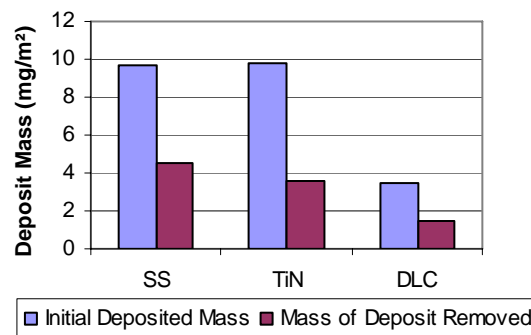

Figure 16: Deposit mass before and after cleaning for SS, TiN & DLC surfaces fouled at 75°C for 10min

DISCUSSION

The findings from the XPS and ellipsometry studies of fouled SS, TiN, and DLC verified that the mechanisms of deposition during the initial stages of fouling are different for the DLC surface. The surface chemistry of this surface was found to be significantly different to the two hydrophilic surfaces and is thus believed to be the main reason for the observed differences. XPS analysis of the fouled SS, TiN, and DLC indicated that similar protein functional groups were present on each surface. However, a key observation in the O components for the DLC surface revealed that the bonding mechanisms may be different in comparison to the SS and TiN. This was found by comparing the high and low intensity components for these surfaces. To elaborate on this point, consider the adsorbed protein molecules. All the functional groups in a protein molecule should be present in the same amount on each surface. However, the bonds formed during adsorption will

depend on the substrate surface chemistry. Thus, the main difference in the adsorbed protein on the different surfaces will be the orientation of the protein. This change in orientation can be detected by the intensity of the various groups. Any functional group that appears to be present at a lower intensity indicates that this group is buried further into the deposit, or in other words, is closer to the interface. For the DLC surface, the low intensity component was the peptide group, indicating that this group was more active during bonding. For the two polar surfaces, the low intensity groups included the carboxyl, C-O, and C-OH groups. By increasing the angle of detection, the XPS scan becomes more surface sensitive resulting in a decrease in concentration from components closer to the interface. Although no definite conclusions could be drawn from the fouled TiN surface, analysis of the fouled DLC surface confirmed that the peptide group is more active during bonding. Angle resolved analysis of fouled SS is currently being performed to determine the bonding mechanisms on this surface, and also to determine whether there are any key differences in initial fouling behaviour between the two polar surfaces.

The ellipsometry study revealed similar findings to the XPS investigation, in that, the mass of deposit for the DLC surface was lower than the deposit mass for the two polar surfaces. The TiN surface appeared to have the highest fouling. Furthermore, it was found that the type of surface not only influenced the rate of deposition, it also influenced the nature of interactions between the initially deposited layer and proteins in the bulk, resulting in a deposit with different removal behaviour. This can be expected, as the change in conformation of the protein when adsorbing to different surfaces will inherently affect the way in which further proteins bond with this initially deposited layer.

From the findings thus far, it is evident that the surface chemistry of the substrate influences the initial stages of fouling to some extent. No significant difference could be found between the two polar surfaces in terms of the orientation of protein functional groups. Both surfaces are expected to influence protein deposition through the oxide layer which defines their surface chemistry. However, it is evident that the amount and rate of fouling is greater for the TiN surface. In biological implants, Ti and TiN are preferred materials due to the bonding behaviour between TiO_2 and biological materials such as blood, tissue and bone (Tosatti et al, 2003; Kola and Daniels, 1996). Hence it is possible that interaction with milk proteins is favourable, since it is the TiO_2 component that is exposed to the solution.

CONCLUSIONS

1. This study investigated the effect of surface modification on the initial stages of fouling.
2. Techniques of XPS and ellipsometry were used to understand the fouling mechanisms of unmodified stainless steel (SS) and stainless steel coated with TiN and DLC.
3. The results presented here do not reveal any significant differences between the SS and TiN surfaces in terms of the orientation of proteins at the surface. As both surfaces are defined by a metal oxide layer, it is possible that bonding mechanisms on these surfaces may be somewhat similar. This is currently under further investigation.
4. Ellipsometry measurements of fouled and cleaned samples revealed that the degree of fouling increased in the order, DLC<SS<TiN, and the cleanability increased in the order TiN<SS<DLC.
5. Deposit removal studies revealed that the nature of surface can influence the structure of the deposit after the initial layer of protein is formed.
6. The key findings from this study suggest that the surface chemistry has an effect on the initial deposition behaviour and deposit removal behaviour to some degree.
7. Further research in this area is expected to lead to the development of specific surfaces that influence the protein bonding mechanisms, and hence combat the problem of fouling.

NOMENCLATURE

Γ adsorbed mass of deposit, mg/m²
d   film or deposit thickness, nm
n   refractive index of film or deposit
A   molar refractivity, cm³/mol
M   molar weight, g/mol

REFERENCES

Azzam, R. M. A. and N. M. Bashara, (1977), Ellipsometry and polarized light. North-Holland, Amsterdam ; Oxford.

Beamson, G. and D. Briggs, (1992), High resolution XPS of organic polymers : the Scienta ESCA300 database. Wiley, New York.

Bertoti, I., M. Mohai, et al., (1995), Surface characterisation of plasma-nitrided titanium: an XPS study, App. Surf. Sci., Vol. 84(4), pp. 357-371.

Beyer, M., T. Felgenhauer, et al., (2006), A novel glass slide-based peptide array support with high functionality resisting non-specific protein adsorption, Biomaterials, Vol. 27(18), pp. 3505-3514.

Bornhorst, A., H. Muller-Steinhagen, et al., (1999), Reduction of Scale Formation Under Pool Boiling Conditions by Ion Implantation and Magnetron Sputtering on Heat Transfer Surfaces, Heat Transfer Eng., Vol. 20(2), pp. 6-14.

Brassart, E. (1990). Chemical interactions at the interface between milk compounds and austenitic stainless steel, University of Lille.

Britten, M., M. L. Green, et al., (1988), Deposit Formation on Heated Surfaces: Effect of Interface Energetics, J. Dairy Res., Vol. 55, pp. 551-562.

Browne, M. M., G. V. Lubarsky, et al., (2004), Protein adsorption onto polystyrene surfaces studied by XPS and AFM, Surf. Sci., Vol. 553(1-3), pp. 155-167.

Changani, S. D., M. T. Belmar-Beiny, et al., (1997), Engineering and Chemical Factors Associated with Fouling and Cleaning in Milk Processing, Exp. Therm. Fluid Sci., Vol. 14(4), pp. 392-406.

Clark, D. T., J. Peeling, et al., (1976), An experimental and theoretical investigation of the core level spectra of a series of amino acids, dipeptides and polypeptides, Biochim. Biophys. Acta, Vol. 453(2), pp. 533-545.

Cuypers, P. A., J. M. M. Kop, et al., (1984), The adsorption of prothrombin to phospholipid monolayers quantitated by ellipsometry, J. Biol. Chem., Vol. 259(22), pp. 13993-13998.

Deplace, F., J. Leuliet, et al., (1994), Fouling experiments of a plate heat exchanger by whey proteins solutions. Proc. Fouling and Cleaning in Food Processing, Jesus College, Cambridge, Vol. pp. 1 - 8

Elofsson, U. M., M. A. Paulsson, et al., (1996), Adsorption during heat treatment related to the thermal unfolding/aggregation of beta-lactoglobulins A and B, J. Colloid Interface Sci., Vol. 183(2), pp. 408-415.

Fortuna, S. V., Y. P. Sharkeev, et al., (2000), Microstructural features of wear-resistant titanium nitride coatings deposited by different methods, Thin Solid Films, Vol. 377-378, pp. 512-517.

Georgiev, D. G., R. J. Baird, et al., (2004), An XPS study of laser-fabricated polyimide/titanium interfaces, App. Surf. Sci., Vol. 236(1-4), pp. 71-76.

Grill, A., (1999), Diamond-like carbon: state of the art, Diamond Relat. Mater., Vol. 8(2-5), pp. 428-434.

Grill, A., (2003), Diamond-like Carbon Coatings as Biocompatible Materials--An Overview, Diamond Relat. Mater., Vol. 12(2), pp. 166-170.

Gyorgy, E., A. Perez del Pino, et al., (2003), Depth profiling characterisation of the surface layer obtained by pulsed Nd:YAG laser irradiation of titanium in nitrogen, Surf. Coat. Technol., Vol. 173(2-3), pp. 265-270.

Hauert, R., (2003), A review of modified DLC coatings for biological applications, Diamond Relat. Mater., Vol. 12(3-7), pp. 583-589.

Khodier, S. A. and H. M. Sidki, (2001), The effect of the deposition method on the optical properties of SiO_2 thin films, J. Mater. Sci. - Mater. Electron., Vol. 12(2), pp. 107-109.

Kola, P. V., S. Daniels, et al., (1996), Magnetron sputtering of tin protective coatings for medical applications, J. Mater. Process. Technol., Vol. 56(1-4), pp. 422-430.

Liu, W., G. K. Christian, et al., (2006), Direct measurement of the force required to disrupt and remove fouling deposits of whey protein concentrate, Int. Dairy J., Vol. 16(2), pp. 164-172.

Lousinian, S. and S. Logothetidis, (2007), Optical properties of proteins and protein adsorption study, Microelectronic Engineering, Vol. 84(3), pp. 479-485.

Lu, F.-H. and H.-Y. Chen, (1999), XPS analyses of TiN films on Cu substrates after annealing in the controlled atmosphere, Thin Solid Films, Vol. 355-356, pp. 374-379.

Milosev, I. and B. Navinsek, (1994), A corrosion study of TiN (physical vapour deposition) hard coatings deposited on various substrates, Surf. Coat. Technol., Vol. 63(3), pp. 173-180.

Milosev, I., H.-H. Strehblow, et al., (1995), XPS in the study of high-temperature oxidation of CrN and TiN hard coatings, Surface & Coatings Technology, Vol. 75(1-3 pt 2), pp. 897-902.

Moulder, J. F. and J. Chastain, (1992), Handbook of x-ray photoelectron spectroscopy : a reference book of standard spectra for identification and interpretation of XPS data. Physical Electronics Division Perkin-Elmer Corp., Eden Prairie, Minn.

Muller-Steinhagen, H. and Q. Zhao, (1997), Investigation of low fouling surface alloys made by ion implantation technology, Chem. Eng. Sci., Vol. 52(19), pp. 3321-3332.

Olivares, O., N. V. Likhanova, et al., (2006), Electrochemical and XPS studies of decylamides of alpha-amino acids adsorption on carbon steel in acidic environment, App. Surf. Sci., Vol. 252(8), pp. 2894-2909.

Parbhu, A. N., J. Soltis, et al., (2004), Specific ion binding influences on surface potential of chromium oxide, Curr. App. Phys., Vol. 4(2-4), pp. 152-155.

Park, J., D.-J. Kim, et al., (2003), Improvement of the biocompatibility and mechanical properties of surgical tools with TiN coating by PACVD, Thin Solid Films, Vol. 435(1-2), pp. 102-107.

Peters, A. M. and M. Nastasi, (2003), Titanium-doped hydrogenated DLC coatings deposited by a novel OMCVD-

PIIP technique, Surf. Coat. Technol., Vol. 167(1), pp. 11-15.

Petoral Jr., R. M. and K. Uvdal, (2002), Arg-Cys and Arg-cysteamine adsorbed on gold and the G-protein-adsorbate interaction, Colloids Surf., B, Vol. 25(4), pp. 335-346.

Piscanec, S., L. Colombi Ciacchi, et al., (2004), Bioactivity of TiN-coated titanium implants, Acta Mater., Vol. 52(5), pp. 1237-1245.

Pradier, C. M., D. Costa, et al., (2002), Role of salts on BSA adsorption on stainless steel in aqueous solutions. I. FT-IRRAS and XPS characterization. Proc. ECASIA'01 Proceedings of the 9th European Conference on Applications of Suface and Interface Analysis, Sep 30-Oct 5 2001, Avignon, France, Vol. 34, pp. 50-54

Robbins, P. T., B. L. Elliott, et al., (1999), A comparison of milk and whey fouling in a pilot scale plate heat exchanger: Implications for Modelling and Mechanistic Studies, Food and Bioproducts Processing: Transactions of the Institution of of Chemical Engineers, Part C, Vol. 77(2), pp. 97-106.

Rosmaninho, R., G. Rizzo, et al., (2003), The Influence of Bulk Properties and Surface Characteristics on the Deposition Process of Calcium Phosphate on Stainless Steel. Proc. Heat Exchanger Fouling and Cleaning Funadmentals and Applications, Sante Fe, New Mexico, USA, Vol. pp.

Rosmaninho, R., O. Santos, et al., (2007), Modified stainless steel surfaces targeted to reduce fouling - Evaluation of fouling by milk components, J. Food Eng., Vol. 80(4), pp. 1176-1187.

Sakiyama, T., K. Tanino, et al., (1999), Adsorption characteristics of tryptic fragments of bovine & beta-lactoglobulin on a stainless steel surface, J. Biosci. Bioeng., Vol. 88(5), pp. 536-541.

Santos, O., T. Nylander, et al., (2006), Effect of surface and bulk solution properties on the adsorption of whey protein onto steel surfaces at high temperature, J. Food Eng., Vol. 73(2), pp. 174-189.

Schmidt, M., (2001), X-ray photoelectron spectroscopy studies on adsorption of amino acids from aqueous solutions onto oxidised titanium surfaces, Archives of Orthopaedic and Trauma Surgery, Vol. 121(7), pp. 403-410.

Sheeja, D., B. K. Tay, et al., (2004), Feasibility of diamond-like carbon coatings for orthopaedic applications, Diamond Relat. Mater., Vol. 13(1), pp. 184-190.

Sundgren, J.-E., (1985), Structure and properties of TiN coatings, Thin Solid Films, Vol. 128(1-2), pp. 21-44.

Tidwell, C. D., D. G. Castner, et al., (2001), Static time-of-flight secondary ion mass spectrometry and x-ray photoelectron spectroscopy characterization of adsorbed albumin and fibronectin films, Surf. Interface Anal., Vol. 31(8), pp. 724-733.

Tosatti, S., S. M. D. Paul, et al., (2003), Peptide functionalized poly(-lysine)-g-poly(ethylene glycol) on titanium: resistance to protein adsorption in full heparinized human blood plasma, Biomaterials, Vol. 24(27), pp. 4949-4958.

Trippe, S. C., R. D. Mansano, et al., (2004), Mechanical properties evaluation of fluor-doped diamond-like carbon coatings by nanoindentation, Thin Solid Films, Vol. 446(1), pp. 85-90.

Valvoda, V., (1996), Structure of TiN coatings, Surf. Coat. Technol., Vol. 80(1-2), pp. 61-65.

Vinnichenko, M., T. Chevolleau, et al., (2002), Spectroellipsometric, AFM and XPS probing of stainless steel surfaces subjected to biological influences, App. Surf. Sci., Vol. 201(1-4), pp. 41-50.

Voros, J., (2004), The density and refractive index of adsorbing protein layers, Biophys. J . Vol. 87(1), pp. 553-561.

Wei, J., D. B. Ravn, et al., (2003), Stainless steel modified with poly(ethylene glycol) can prevent protein adsorption but not bacterial adhesion, Colloids Surf., B, Vol. 32(4), pp. 275-291.

Xiao, S. J., M. Textor, et al., (1997), Immobilization of the cell-adhesive peptide Arg-Gly-Asp-Cys (RGDC) on titanium surfaces by covalent chemical attachment, J. Mater. Sci. Mater. Med., Vol. 8(12), pp. 867-872.

Zettler, H. U., M. Wiess, et al., (2005), Influence of surface properties and characteristics on fouling in plate heat exchangers, Heat Transfer Eng., Vol. 26(2), pp. 3-17.

Zhang, W., Y. Li, et al., (2004), Influence of argon flow rate on TiO_2 photocatalyst film deposited by dc reactive magnetron sputtering, Surf. Coat. Technol., Vol. 182(2-3), pp. 192-198.

Zhao, J., E. G. Garza, et al., (2000), Comparison study of physical vapor-deposited and chemical vapor-deposited titanium nitride thin films using X-ray photoelectron spectroscopy, App. Surf. Sci., Vol. 158(3-4), pp. 246-251.

Zhao, Q. and Y. Liu, (2004), Investigation of graded Ni-Cu-P-PTFE composite coatings with antiscaling properties, App. Surf. Sci., Vol. 229(1-4), pp. 56-62

Zubavichus, Y., O. Fuchs, et al., (2004), Soft X-ray-induced decomposition of amino acids: An XPS, mass spectrometry, and NEXAFS study, Radiat. Res., Vol. 161(3), pp. 346-358.